MOX-Report No. 30/2017

Parameter identification for the linear wave equation with Robin boundary condition

Bacchelli, V.; Micheletti, S.; Perotto, S.; Pierotti, D.

MOX, Dipartimento di Matematica
Politecnico di Milano, Via Bonardi 9 - 20133 Milano (Italy)

mox-dmat@polimi.it http://mox.polimi.it

Parameter identification for the linear wave equation with Robin boundary condition

Valeria Bacchelli*, Stefano Micheletti#, Simona Perotto# and Dario Pierotti*

June 14, 2017

MOX– Modellistica e Calcolo Scientifico
Dipartimento di Matematica, Politecnico di Milano
Piazza L. da Vinci 32, I-20133 Milano, Italy
{stefano.micheletti,simona.perotto}@polimi.it

* Dipartimento di Matematica, Politecnico di Milano
Piazza L. da Vinci 32, I-20133 Milano, Italy
{valeria.bacchelli,dario.pierotti}@polimi.it

2010 Mathematics Subject Classification: 35L05, 35L20, 35C05, 35R30, 65M60, 65L09
Keywords: Wave equation, method of characteristics, solutions in closed form, parameter estimation, stability analysis, finite element method, Newmark method

Dedicated to Fausto

Abstract

We consider an initial-boundary value problem for the classical linear wave equation, where mixed boundary conditions of Dirichlet and Neumann/Robin type are enforced at the endpoints of a bounded interval. First, by a careful application of the method of characteristics, we derive a closed-form representation of the solution for an impulsive Dirichlet data at the left endpoint, and valid for either a Neumann or a Robin data at the right endpoint. Then we devise a reconstruction procedure for identifying both the interval length and the Robin parameter. We provide a corresponding stability result and verify numerically its performance moving from a finite element discretization.

1 Introduction

Let us consider the following mixed boundary value problem for the wave equation

$$\begin{cases} u_{xx} - u_{tt} = 0 & 0 < x < b,\ t > 0, \\ u(x,0) = 0 & 0 < x < b, \\ u_t(x,0) = 0 & 0 < x < b, \\ u(0,t) = h(t) & t \geq 0, \\ u_x(b,t) + \gamma u(b,t) = 0 & t \geq 0, \end{cases} \tag{1}$$

where $b > 0$, $\gamma \geq 0$, and $h(t)$ a $\mathcal{C}^1$ function in $[0, +\infty)$ such that $h(0) = 0$ are assigned data. The above system, though pretty simple, actually models some physical problems of interest in engineering applications. For instance, the unknown function, $u(x,t)$, describes the transverse vibrations of a string of finite length, with respect to the horizontal rest configuration, with vertical component of the tension given by $u_x(x,t)$. In this context, Dirichlet, Neumann and Robin boundary conditions have a direct physical interpretation. In particular, a null Neumann data, $u_x(b,t) = 0$, is associated with a free transverse motion, i.e., no external transverse force acts on this end; a homogeneous Robin condition, $u_x(b,t) + \gamma u(b,t) = 0$, represents a linearly restorative transverse force, that is, the end is transversally restrained, but elastically rather than rigidly [11]. For this reason, this last condition is often referred to as elastic.

Another relevant application of the wave equation is in acoustics, where u is the velocity potential associated with the propagation of a pressure wave in a carrier medium [1]. The Dirichlet boundary condition on a certain surface, for a complex amplitude pressure, is applied when the material of the surface has very low acoustic impedance compared to that of the medium. In this case the surface is called sound soft. Vice versa, when the surface material has much higher acoustic impedance than the one of the host medium, a Neumann boundary condition holds, and the surface is called sound hard. The Robin (or impedance) boundary condition models finite acoustic impedance, γ being proportional to the admittance of the surface.

We suppose that the boundary, $x = b$, is unknown and inaccessible, whereas $x = 0$ is accessible for input and output measurements. Then, we deal with the inverse problem of determining b and γ, provided additional measurements, $u_x(0,t)$, are known, for t in the bounded interval $(0, t_f)$.

An analogous problem was considered in spatial dimension $d \geq 2$ by Isakov [7], assuming that the unknown boundary Γ is a closed *polygonal surface*. The author proved that an additional measurement of the normal derivative on the known part of the boundary for large enough t_f uniquely determines Γ and γ. Moreover, inverse problems involving a Robin condition in a *parabolic* equation was considered in [2]. The authors prove that two pairs of measurements guarantee uniqueness and stability of both Γ and γ. In the context of hyperbolic problems, although addressing a different identification problem, it is worth mentioning the following works. In [12], the wave equation is considered where the spa-

tial operator is in conservation form, $(K(x)\,u_x)_x$, and the problem is set on the half line, $x > 0$. An inverse problem for the identification of the coefficient $K(x)$ is proposed, based on the boundary impulse response, i.e., by measuring the function $u(x,0) = f(t)$ associated with the Neumann boundary condition, $u_x(0,t) = \delta(t)$. A similar problem in addressed in [9], where the inverse medium problem associated with the reconstruction of the heterogeneous material profile of a semi-infinite layered soil medium, directly in the time domain, is studied. The method is based on the complete waveform response of the medium to a forcing Neumann boundary condition on the surface. The inversion process relies on a partial differential equation constrained optimization approach, supplemented with a time-dependent regularization scheme. An absorbing boundary condition is enforced at the bottom of the domain, at a certain depth, to take into account the artificial truncation of the spatial domain. Moreover, for the case when there is no homogeneous bottom layer, or its precise location is not a priori known, the authors propose two iterative schemes to identify the domain depth. A force identification problem for the wave equation is studied in [8], where the space-dependent part of the source term is recovered from measurements of the final or time-average displacement of the wave.

In this paper, we uniquely identify the pair (b, γ) by evaluating the output flux, $u_x(0,t)$, of the solution generated by an *impulsive Dirichlet data*, $h(t)$, for a sufficiently large time interval. We also provide a stability estimate. A key point is the determination of the closed-form solution to (1), at least up to a definite time, but in principle extendable to any larger time. This is carried out by a clever usage of the method of characteristics, which we exploit to build the solution in space-time triangular domains. Clearly, the domain of dependence of u at a given space-time point, say $(\bar{x}, \bar{t})$, is the interval $[\bar{x} - \bar{t}, \bar{x} + \bar{t}]$, whose width increases with $\bar{t}$, making the procedure more involved. On the other hand, as far as we know, for $\gamma \neq 0$, a closed-form global-in-time solution is not available.

Then, the performance of the identification procedure is tested numerically. We devise an algorithm which takes into account the unavoidable approximations and smoothing effects introduced by the numerical discretization. In particular, the wave equation is dealt with a Galerkin finite element method with polynomial approximation of arbitrary degree for the spatial variable, and a Newmark method to advance in time. The impulsive Dirichlet data is approximated by a Gaussian function of unit area and with a very small variance. The overall scheme is unconditionally stable (with a proper selection of the parameters in the Newmark method), and we show that one can obtain a very accurate reconstruction of the physical parameters. Actually, very small space and time discretization steps are required to describe the sharp Gaussian profile and to reduce the dispersion error of the method.

The paper is organized as follows. In Section 2, we exploit the method of characteristics to obtain an explicit representation (for some bounded time interval) of the solution to (1) with $h(t) = \delta(t - t_0)$, $t_0 > 0$. In Section 3, we first define a function $g(T)$ by a suitable weighted integral on $(0, T)$ of the

output flux $u_x(0,t)$; then, we show that the study of g allows us to uniquely determine the pair (b,γ) (see Proposition 3.1). Finally, the stability is discussed by defining an appropriate notion of distance between a pair of such functions g. In Section 4, we introduce the numerical algorithm employed to assess the robusteness and accuracy of the identification procedure. Some conclusions are drawn in Section 5.

2 A representation formula of the solution

As it is known, problem (1) has a unique classical solution $u \in \mathcal{C}^2\big((0,b)\times(0,+\infty)\big)\cap\mathcal{C}^1\big([0,b]\times(0,+\infty)\big)$ [6]. We provide here a closed-form representation of the solution on a specific bounded time interval.

Proposition 2.1 *A representation of the flux, $u_x(0,t)$, valid in the interval $0<t<3b$, is provided by*

$$u_x(0,t) = -h'(t) \tag{2}$$
$$+\begin{cases} 0 & 0<t<2b \\ 2h'(t-2b) - 4\gamma h(t-2b) + 4\gamma^2 e^{-\gamma(t-2b)}\int_0^{t-2b} e^{\gamma s}h(s)\,ds & 2b<t<3b. \end{cases}$$

Proof. This proof is based on a repeated application of the method of characteristics [4]. With this aim, it is enough to obtain an explicit expression for the solution in the triangles T_0, and T_2 in Fig. 1. As it should be clear from this picture, for the evaluation of the solution in T_2, we need to compute the solution also in T_1, where the influence of the Robin boundary condition first appears. Then, we divide the proof into three steps, by processing each triangle in turn.

Solution in T_0. We observe that the solution u is vanishing for $0\le x\le b$ and $0\le t\le x$, while in the triangle T_0, defined by

$$T_0 := \{0\le x\le b,\quad x\le t\le 2b-x\},$$

we simply have

$$u(x,t) = h(t-x).$$

Hence,

$$u_x(0,t) = -h'(t) \qquad \text{for} \qquad 0\le t<2b.$$

Solution in T_1. We now represent the solution $u(x,t)$ in the triangle

$$T_1 := \{b/2\le x\le b,\quad 2b-x\le t\le x+b\}.$$

Then, thanks to the d'Alembert formula, we write the solution in T_1 in the form

$$u(x,t) = \frac{1}{2}\phi(x-t+b) + \frac{1}{2}\phi(x+t-b) + \frac{1}{2}\int_{x-t+b}^{x+t-b}\psi(s)\,ds, \tag{3}$$

where ϕ, ψ are the Cauchy data at $t=b$, which depend on the solution at previous times. Clearly, in the interval $0\le x\le b$, we have $\phi(x)=h(b-x)$, and $\psi(x)=h'(b-x)$. Additionally, to define (3) for $(x,t)\in T_1$, it is necessary to specify the data ϕ, ψ in the

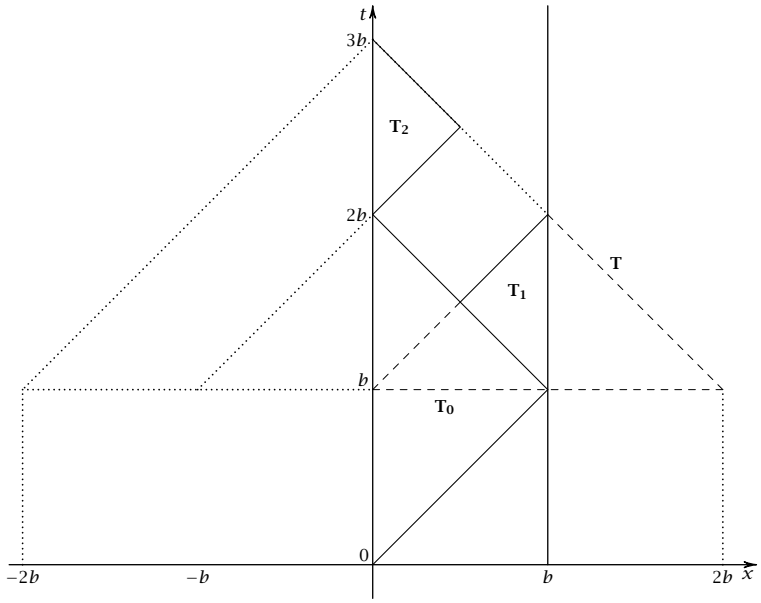

Figure 1: Graphic representation of the method of characteristics.

whole interval $0 \leq x \leq 2b$. This can be accomplished by exploiting the Robin boundary condition.

For this purpose, we re-write (3) as

$$u(x,t) = \frac{1}{2}h(t-x) + \frac{1}{2}\phi(x+t-b) + \frac{1}{2}\int_{x-t+b}^{b} h'(b-s)\,ds + \frac{1}{2}\int_{b}^{x+t-b} \psi(s)\,ds.$$

By explicitly integrating the third term, and since $h(0) = 0$, we have

$$u(x,t) = h(t-x) + H(t+x-b), \tag{4}$$

where

$$H(\xi) = \frac{1}{2}\phi(\xi) + \frac{1}{2}\int_{b}^{\xi} \psi(s)\,ds \qquad b \leq \xi \leq 2b.$$

We now determine the unknown function H by imposing the boundary condition $u_x(b,t) + \gamma u(b,t) = 0$. We obtain the Cauchy problem:

$$\begin{cases} H'(t) + \gamma H(t) = h'(t-b) - \gamma h(t-b) & t > b, \\ H(b) = \frac{1}{2}\phi(b) = \frac{1}{2}h(0) = 0. \end{cases}$$

The solution to this problem is provided by

$$H(t) = h(t-b) - 2\gamma e^{-\gamma(t-b)} \int_{0}^{t-b} e^{\gamma s} h(s)\,ds = h(t-b) - 2\gamma \tilde{h}(t-b),$$

where

$$\tilde{h}(\xi) := e^{-\gamma\xi} \int_{0}^{\xi} e^{\gamma s} h(s)\,ds. \tag{5}$$

Note that $\tilde{h}' = h - \gamma\tilde{h}$. By plugging the expression of H into (4), we obtain

$$u(x,t) = h(t-x) + h(t+x-2b) - 2\gamma\tilde{h}(t+x-2b), \tag{6}$$

for $(x,t) \in T_1$.

We now determine the functions ϕ, ψ, in (3). Let us consider the triangle

$$T := \{b \le t \le 2b, \quad t-b \le x \le 3b-t\},$$

which includes T_1, part of T_0, and a part of the half-plane $x > b$ (see Fig. 1). By (6), and since $u(x,t) = h(t-x)$ in T_0, it can be easily checked that u coincides with the solution (still denoted by u) of the wave equation in T with Cauchy data at $t = b$ given by

$$u(x,b) = \begin{cases} h(b-x) & 0 \le x \le b, \\ h(x-b) - 2\gamma\tilde{h}(x-b) & b \le x \le 2b, \end{cases} \tag{7}$$

and

$$u_t(x,b) = \begin{cases} h'(b-x) & 0 \le x \le b, \\ h'(x-b) - 2\gamma h(x-b) + 2\gamma^2\tilde{h}(x-b) & b \le x \le 2b. \end{cases} \tag{8}$$

By comparison with (3), it follows that the right-hand side of (7) and of (8) are the required functions ϕ, ψ in $b \le x \le 2b$.

Solution in T_2. We can now go further, by evaluating the solution in the upper triangle

$$T_2 := \{0 \le x \le b/2, \quad 2b + x \le t \le 3b - x\}.$$

With this aim, we still employ the d'Alembert formula to represent the solution as

$$u(x,t) = \frac{1}{2}\phi(x-t+b) + \frac{1}{2}\phi(x+t-b) + \frac{1}{2}\int_{x-t+b}^{x+t-b} \psi(s)\,ds.$$

However, since $(x,t) \in T_2$, the initial values at $t = b$ have to be defined in the larger interval $-2b \le x \le 2b$. Using (7) and (8), and since, for $(x,t) \in T_2$, one has $-2b \le x - t + b \le -b$ and $b \le x + t - b \le 2b$, it holds

$$u(x,t) = K(x-t+b) + \frac{1}{2}\Big[h(x+t-2b) - 2\gamma\tilde{h}(x+t-2b)\Big]$$
$$+\frac{1}{2}\int_0^b h'(b-s)\,ds + \frac{1}{2}\int_b^{x+t-b} \big[h'(s-b) - 2\gamma h(s-b) + 2\gamma^2\tilde{h}(s-b)\big]\,ds,$$

where

$$K(\xi) := \frac{1}{2}\phi(\xi) + \frac{1}{2}\int_\xi^0 \psi(s)\,ds \qquad -2b \le \xi \le 0.$$

By explicit integration of the terms containing h', we obtain

$$\begin{aligned} u(x,t) &= K(x-t+b) + \frac{1}{2}h(b) + h(x+t-2b) - \gamma\tilde{h}(x+t-2b) \\ &- \gamma\int_0^{x+t-2b} h(s)\,ds + \gamma^2\int_0^{x+t-2b} \tilde{h}(s)\,ds. \end{aligned} \tag{9}$$

To determine the unknown function K, we enforce the Dirichlet condition $u(0,t) = h(t)$, for $t \ge b$, so that

$$K(b-t) + \frac{1}{2}h(b) + h(t-2b) - \gamma\tilde{h}(t-2b) - \gamma\int_0^{t-2b} h(s)\,ds + \gamma^2\int_0^{t-2b} \tilde{h}(s)\,ds = h(t).$$

By solving for K, and by replacing t with $t-x$, we have

$$\begin{aligned} K(x-t+b) &= h(t-x) - \frac{1}{2}h(b) - h(t-x-2b) + \gamma\tilde{h}(t-x-2b) \\ &+ \gamma\int_0^{t-x-2b} h(s)\,ds - \gamma^2\int_0^{t-x-2b}\tilde{h}(s)\,ds. \end{aligned}$$

Finally, using this expression in (9), we obtain

$$\begin{aligned} u(x,t) = h(t-x) + h(x+t-2b) - h(t-x-2b) \\ -\gamma[\tilde{h}(x+t-2b) - \tilde{h}(t-x-2b)] - \gamma\int_{t-x-2b}^{t+x-2b} h(s)\,ds + \gamma^2\int_{t-x-2b}^{t+x-2b}\tilde{h}(s)\,ds, \end{aligned}$$

where $\tilde{h}$ is given by (5), with $0 \le x \le b/2$, $2b+x \le t \le 3b-x$. Hence, by recalling that $\tilde{h}' = h - \gamma\tilde{h}$, we obtain

$$u_x(0,t) = -h'(t) + 2h'(t-2b) - 4\gamma h(t-2b) + 4\gamma^2\tilde{h}(t-2b) \qquad 2b < t < 3b,$$

so that (2) is proved. □

3 The inverse problem

Suppose $0 < b_0 \le b$, $\gamma \ge 0$. The inverse problem of interest consists in determining uniquely b and γ, by choosing a suitable input $h(t)$ and by measuring the output flux, $u_x(0,t)$, namely, we aim to recover the unknown pair $(b,\,\gamma)$ by measuring the flux at $x=0$ generated by an impulse at time t_0.

By inserting in the representation (2) the impulse

$$h(t) = \delta(t-t_0), \tag{10}$$

where $t_0 > 0$ is a suitable small time, we have

$$\begin{aligned} u_x(0,t) &= -\delta'(t-t_0) + 2\delta'\big(t-(2b+t_0)\big) \\ &\quad -4\gamma\delta\big(t-(2b+t_0)\big) + 4\gamma^2 e^{-\gamma(t-(2b+t_0))}\,\mathbf{1}_{(2b+t_0,3b)}(t), \end{aligned} \tag{11}$$

where $0 < t < 3b$ and $\mathbf{1}_{(a,b)}$ denotes the indicator function of the interval (a,b).

Clearly, equation (11) holds in the distribution sense, and can be obtained as the limiting solution to a regularized version of (2), associated with a sequence $\{h_n(t)\}$ of boundary data, such that $h_n(t) \to \delta(t-t_0)$ (e.g., a sequence of Gaussian functions centered at t_0). Then, we will take as output boundary data some weighted integral of (11) with test function *supported in the interval* $[0,3b)$. The presence of the derivatives of the delta function in (11) leads to using $\mathcal{C}^1$ weight functions (i.e., we can not simply integrate the output flux on some interval $[0,T] \subset [0,3b)$). However, piecewise smooth, continuous functions can be chosen too. Thus, for every $T \ge b_0/2$, we consider the continuous, piecewise linear function

$$\varphi_T(t) := \begin{cases} 1 & 0 \le t \le T - \frac{b_0}{2} \\ \frac{2}{b_0}(T-t) & T - \frac{b_0}{2} \le t \le T \\ 0 & t \ge T. \end{cases} \tag{12}$$

Assume further that $t_0 < \frac{b_0}{2}$ and $t_0 + \frac{b_0}{2} \le T < 3b$. Then, we define

$$g(T) := \int_0^T u_x(0,t)\,\varphi_T(t)dt, \tag{13}$$

with $u_x(0,t)$ as in (11). Note that, the integral can be extended to the interval $[0, 3b)$ by exploiting the bounded support of φ_T.

By the properties of the delta function and of its derivative, we obtain:

$$g(T) = \begin{cases} 0 \qquad \text{for } t_0 + \dfrac{b_0}{2} \le T < 2b + t_0, \\ \dfrac{4}{b_0} - \dfrac{8\gamma}{b_0}(T - (2b+t_0)) + \dfrac{8\gamma^2}{b_0}\displaystyle\int_{2b+t_0}^{T} s(t)(T-t)\,dt \\ \qquad \text{for } 2b + t_0 < T < 2b + t_0 + \dfrac{b_0}{2}, \\ -4\gamma + 4\gamma^2 \displaystyle\int_{2b+t_0}^{T-\frac{b_0}{2}} s(t)dt + \dfrac{8\gamma^2}{b_0}\displaystyle\int_{T-\frac{b_0}{2}}^{T} s(t)(T-t)\,dt \\ \qquad \text{for } 2b + t_0 + \dfrac{b_0}{2} < T \le 3b, \end{cases}$$

where, to simplify notation, we set $s(t) = e^{-\gamma(t-(2b+t_0))}$. Then, by explicit evaluation of the integrals, we get

$$g(T) = \begin{cases} 0 & \text{for } t_0 + \dfrac{b_0}{2} \le T < 2b + t_0 \\ \dfrac{4}{b_0}(2s(T) - 1), & \text{for } 2b + t_0 < T < 2b + t_0 + \dfrac{b_0}{2} \\ -\dfrac{8}{b_0} s(T)\,(e^{\gamma\frac{b_0}{2}} - 1), & \text{for } 2b + t_0 + \dfrac{b_0}{2} < T \le 3b. \end{cases} \tag{14}$$

Function g is not defined at $T = 2b + t_0$ and $T = 2b + t_0 + \frac{b_0}{2}$, where it exhibits discontinuities, due to the jumps of the (weak) derivative of φ_T. In particular, at $T = 2b + t_0$ we have

$$g(2b + t_0)^- = 0, \qquad g(2b + t_0)^+ = \frac{4}{b_0}.$$

Then g decreases until reaching the second discontinuity, at $T = 2b + t_0 + \frac{b_0}{2}$, where

$$g\big(2b + t_0 + \frac{b_0}{2}\big)^- = \frac{4}{b_0}(2e^{-\gamma\frac{b_0}{2}} - 1), \qquad g\big(2b + t_0 + \frac{b_0}{2}\big)^+ = -\frac{8}{b_0}(1 - e^{-\gamma\frac{b_0}{2}}) < 0.$$

Finally, g increases, still remaining negative for larger T (see Fig. 2 for an example). Notice that, either the abscissa $2b + t_0$ or $2b + t_0 + b_0/2$ of the points of

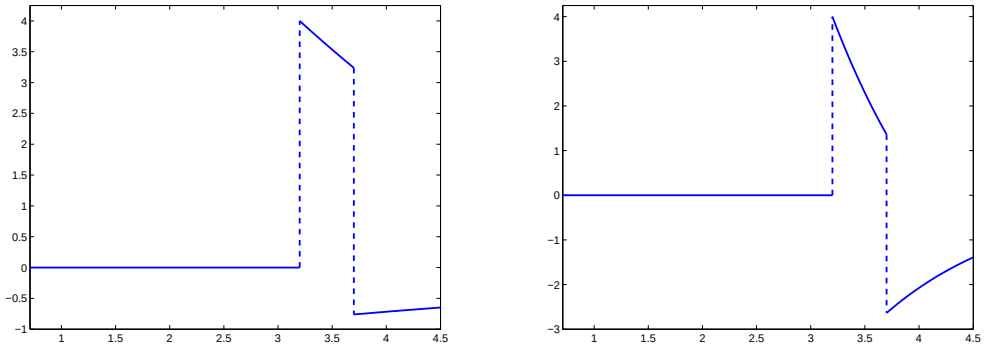

Figure 2: Plot of g for $b_0 = 1$, $b = 1.5$, $t_0 = 0.2$, $\gamma = 0.2$ (left) and $\gamma = 0.8$ (right).

discontinuity *uniquely* determines the length b.

Now, in order to determine γ, it is convenient to *extend g to a right-continuous function* (still denoted by g) for $T \in [0, 3b)$, that is

$$g(2b + t_0) = g\big(2b + t_0\big)^+, \qquad g(2b + t_0 + \frac{b_0}{2}) = g\big(2b + t_0 + \frac{b_0}{2}\big)^+. \tag{15}$$

Then, $g(T)$ assumes *maximum value* $g(2b + t_0) = \frac{4}{b_0}$ and *minimum value*

$$g(2b + t_0 + \frac{b_0}{2}) = -\frac{8}{b_0}(1 - e^{-\gamma \frac{b_0}{2}}) := -\Delta. \tag{16}$$

The maximum is independent of the unknowns b and γ (and equals the jump at both discontinuities, see Fig. 2), while the minimum depends only on γ, so that γ can be uniquely determined as

$$\gamma = -\frac{2}{b_0} \ln\Big(1 - \frac{\Delta b_0}{8}\Big). \tag{17}$$

Note that Δ is also equal to the value of the gap

$$g(2b + t_0) - g(2b + t_0 + \frac{b_0}{2})^- = \frac{8}{b_0}\big(1 - e^{-\gamma b_0/2}\big).$$

We can sum up the previous discussion in the following

Proposition 3.1 *Let $u(x,t)$ be the (weak) solution to (1) with Dirichlet data $u(0,t) = \delta(t - t_0)$, and assume that the endpoint b and the parameter γ in (1) satisfy $b \geq b_0 > 0$, $\gamma \geq 0$ and that $0 < t_0 < b_0/2$. Moreover, let g be the right-continuous function defined by (13)-(15). Then, denoting by T_M the abscissa of the unique maximum of g, we have*

$$b = \frac{1}{2}(T_M - t_0). \tag{18}$$

Furthermore, the parameter γ is determined by

$$\gamma = -\frac{2}{b_0} \ln\Big(1 + \frac{g_m b_0}{8}\Big). \tag{19}$$

where $g_m = g(T_M + b_0/2)$ is the minimum value of g.

According to the above proposition, the unknown pair (b, γ) is recovered by evaluating the weighted integrals (13) of the output flux up to the time $T_M + b_0/2$.

Remark 3.1 *If an upper bound, $b < \bar{b}$, is known a priori, the flux could be evaluated up to a maximum time, $T = 2\bar{b} + t_0 + b_0/2$.*

Notice that the value of γ is determined regardless of b. This property could be exploited to improve the evaluation of b.

For, let us suppose that the points of discontinuity are known to lie in the interval $(\overline{T} - \epsilon, \overline{T} + \epsilon)$ and $(\overline{T} + b_0/2 - \epsilon, \overline{T} + b_0/2 + \epsilon)$, respectively, where $0 < \epsilon < b_0/4$ (this means that $\frac{1}{2}(\overline{T} - t_0 - \epsilon) < b < \frac{1}{2}(\overline{T} - t_0 + \epsilon)$). Then, after computing γ as in (17), choose

$$T_M \in (\overline{T} + \epsilon,\, \overline{T} + \frac{b_0}{2} - \epsilon)$$

and measure the value $g(T_M)$. Since T_M lies between the points of discontinuity, by (14), we readily obtain

$$b = \frac{1}{2}(T_M - t_0) + \frac{1}{2\gamma} \ln\Big[\frac{1}{2} + \frac{b_0}{8} g(T_M)\Big].$$

The above formula could be used to provide a better estimate of b provided that γ and $g(T_M)$ are determined with sufficient precision (see below).

Remark 3.2 (The case of the Neumann condition) *It could be interesting to consider the case $\gamma = 0$ in (1), that is to uniquely determine b when the homogeneous Neumann condition $u_x(b, t) = 0$ is assigned. By setting $\gamma = 0$ in (14), it turns out that*

$$g(T) = \frac{4}{b_0}\, \mathbf{1}_{(2b+t_0,\, 2b+t_0+b_0/2)},$$

so that the unknown b is determined by locating the discontinuities of g, which degenerates to a rectangle function.

Remark 3.3 *One could also choose any scaled version $m\varphi_T$ of the test function in (12), with $m > 0$. In such a case, function g scales accordingly, while (17) still holds with Δ defined by (16).*

3.1 Stability analysis

We have shown that, if u is the solution of (1) with impulsive Dirichlet data at $x = 0$, then the function g defined in Proposition 3.1 uniquely determines the parameters (b, γ). We now discuss the stability of such reconstruction procedure. Hence, we will estimate the distance between two points in the plane (b, γ) in terms of some suitably defined distance between two functions g. With this aim, notice that:

- by (19), the parameter γ is uniquely determined by the minimum value of g;
- by extending $g(T)$ to zero outside the interval $(t_0 + b_0/2, 3b)$, the graphs of two functions with the same γ and $b = b_1$, $b = b_2$ differ by a shift of $b_2 - b_1$ along the T axis.

Let us now define $g_{\{b,\gamma\}} : \mathbb{R} \to \mathbb{R}$ be the extension to zero of $g(T)$ given by (14). For any $b \geq b_0 > 0$ and $\gamma \geq 0$, the function $g_{\{b,\gamma\}}$ is bounded and compactly supported.

Thanks to the two previous remarks, we define the distance:

$$\begin{aligned} d\big(g_{\{b_1,\gamma_1\}}, g_{\{b_2,\gamma_2\}}\big) \;&:=\; \int_{\mathbb{R}} \big|g_{\{b_1,\gamma_1\}}(T) - g_{\{b_2,\gamma_2\}}(T)\big|\, dT \\ &+\; \big|\inf_T g_{\{b_1,\gamma_1\}}(T) - \inf_T g_{\{b_2,\gamma_2\}}(T)\big|, \end{aligned} \tag{20}$$

where the right-hand side is well defined in the set $G \times G$, where

$$G := \Big\{ g_{\{b,\gamma\}},\ (b,\gamma) \in [b_0, +\infty) \times [0, +\infty) \Big\}. \tag{21}$$

Then, we prove the following stability result.

Theorem 3.1 *Let $g_{\{b,\gamma\}}$ be defined as above and assume that $b \geq b_0 > 0$ and $0 \leq \gamma \leq \bar{\gamma}$, for some $\bar{\gamma} > 0$. Then, there exist positive constants, C, η, depending only on b_0, $\bar{\gamma}$, such that*

$$d\big(g_{\{b_1,\gamma_1\}}, g_{\{b_2,\gamma_2\}}\big) \geq C\big(|b_1 - b_2| + |\gamma_1 - \gamma_2|\big), \tag{22}$$

whenever $|b_1 - b_2| \leq \eta$.

Proof. Let Δ_1, Δ_2 be defined as in (16), for $\gamma = \gamma_1$ and $\gamma = \gamma_2$, respectively. By (17) and simple calculus, we have

$$|\gamma_1 - \gamma_2| = \frac{2}{8 - b_0\,\tilde{\Delta}} |\Delta_1 - \Delta_2|,$$

where $\Delta_1 < \tilde{\Delta} < \Delta_2$. By (16) and exploiting the bound on γ, we obtain $\tilde{\Delta} \leq \bar{\Delta} < 8/b_0$, with $\bar{\Delta}$ as in (16) for $\gamma = \bar{\gamma}$, so that

$$|\gamma_1 - \gamma_2| \leq \frac{2}{8 - b_0\,\bar{\Delta}} |\Delta_1 - \Delta_2|. \tag{23}$$

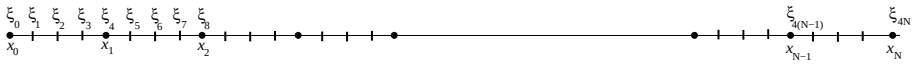

Figure 3: Degrees of freedom and nodes associated with the space U^r_σ, for $r = 4$.

Suppose now that $b_1 < b_2 \leq b_1 + b_0/4$, and consider the function $g_1 - g_2$, where we set $g_1 = g_{\{b_1,\gamma_1\}}$, $g_2 = g_{\{b_2,\gamma_2\}}$.
Note that, in the interval $2b_1 + t_0 \leq T < 2b_2 + t_0$, one has

$$g_1(T) = \frac{4}{b_0}(2e^{-\gamma_1(T-(2b_1+t_0))} - 1) \qquad \text{and} \qquad g_2(T) = 0.$$

Moreover, g_1 is decreasing in $2b_1 + t_0 \leq T < 2b_2 + t_0$, with

$$g_1(2b_2 + t_0) = \frac{4}{b_0}(2e^{-2\gamma_1(b_2-b_1)} - 1) \geq \frac{4}{b_0}(2e^{-2\bar\gamma(b_2-b_1)} - 1).$$

The last term is positive provided that

$$b_2 - b_1 < \frac{1}{2\bar\gamma}\ln 2.$$

Hence, by defining

$$\eta := \min\Big\{\frac{b_0}{4}, \frac{\ln 2}{2\bar\gamma}\Big\},$$

it holds, for $|b_1 - b_2| < \eta$,

$$\int_{\mathbb{R}} \big|g_1(T) - g_2(T)\big|\, dT > \int_{2b_1+t_0}^{2b_2+t_0} \big|g_1(T)\big|\, dT \geq \frac{8K}{b_0}|b_1 - b_2|, \tag{24}$$

where the positive constant K depends only on $\bar\gamma$ and η. Recalling that $\Delta_i = -\inf_T g_i(T)$, with $i = 1, 2$, result (22) follows by estimates (23) and (24), and by choosing $C = \min\big\{8K/b_0, (8 - b_0\,\bar\Delta)/2\big\}$. □

4 The discrete problem

We consider the discretization of problem (1). In particular, since we are dealing with a space-time problem, we first discretize in space via a finite element scheme, and then in time, by resorting to the Newmark method.
Let us start by subdividing the domain $[0, b]$ into N uniform sub-intervals via the $N + 1$ nodes $\{x_i\}_{i=0}^N$, with $x_{i+1} = x_i + \sigma$, with $\sigma = b/N$, $x_0 = 0$ and $x_N = b$. With a view to the finite element approximation, we introduce the finite dimensional space $U^r_\sigma = \{w \in C^0([0, b]) : w|_{[x_i,x_{i+1}]} \in \mathbb{P}^r\}$, of piecewise continuous function of degree r, whose corresponding degrees of freedom are denoted by ξ_j, $j = 0, \ldots, rN$, following the ordering described in Fig. 3. Thus, the semi-discrete finite element approximation is: $\forall t > 0$, find $u^\sigma(t) \in U^r_\sigma$ such that, $\forall v^\sigma \in V^r_\sigma$,

$$\int_0^b u^\sigma_{tt}(x,t)v^\sigma(x)\, dx + \int_0^b u^\sigma_x(x,t)v^\sigma_x(x)\, dx + \gamma u^\sigma(b,t)v^\sigma(b) = 0, \tag{25}$$

with $u^\sigma(0,t) = h(t)$, $u^\sigma(x,0) = u_t^\sigma(x,0) = 0$, and where $V_\sigma^r = \{w \in U_\sigma^r : w(0,t) = 0 \ \forall t > 0\}$. Notice also that we adopt the standard convention of omitting the dependence on x when, at a given time, functions are meant in U_σ^r. The algebraic counterpart of (25) is provided by the following system of ordinary differential equations:

$$\begin{cases} \widetilde{M}\tilde{\mathbf{u}}_{tt}(t) + \widetilde{K}\tilde{\mathbf{u}}(t) &= \mathbf{0} \quad t > 0 \\ \tilde{\mathbf{u}}(0) &= \mathbf{0} \\ \tilde{\mathbf{u}}_t(0) &= \mathbf{0}, \end{cases} \tag{26}$$

with $\tilde{\mathbf{u}}(t) = \{u^\sigma(\xi_i,t)\}_{i=0}^{rN} \in \mathbb{R}^{rN+1}$, $\widetilde{M} = [\tilde{m}_{ij}]_{i,j=0}^{rN} \in \mathbb{R}^{(rN+1)\times(rN+1)}$, $\widetilde{K} = [\tilde{k}_{ij}]_{i,j=0}^{rN} \in \mathbb{R}^{(rN+1)\times(rN+1)}$, with

$$\tilde{m}_{ij} = \int_0^b \phi_i(x)\,\phi_j(x)\,dx, \quad \tilde{k}_{ij} = \int_0^b \phi_{i,x}(x)\,\phi_{j,x}(x)\,dx + \gamma\delta_{i,rN}\delta_{j,rN},$$

the elements of the mass and of the stiffness matrix, respectively, $\delta_{k,rN}$ being the Kronecker symbol, $u^\sigma(\xi_0,t) = h(t)$, and with $\{\phi_k\}_{k=0}^{rN}$ the finite element basis functions, assumed to be Lagrangian, so that $u^\sigma(x,t) = \sum_{k=0}^{rN} u^\sigma(\xi_k,t)\phi_k(x)$. System (26) can be reduced in dimension in order to highlight the known quantities as

$$\begin{cases} M\mathbf{u}_{tt}(t) + K\mathbf{u}(t) &= -\big(h(t)\,\mathbf{f} + h_{tt}(t)\,\mathbf{m}\big) =: \mathbf{F}(t) \quad t > 0 \\ \mathbf{u}(0) &= \mathbf{0} \\ \mathbf{u}_t(0) &= \mathbf{0}, \end{cases} \tag{27}$$

where[1] $K = \widetilde{K}(2 : rN+1, 2 : rN+1) \in \mathbb{R}^{rN\times rN}$, $M = \widetilde{M}(2 : rN+1, 2 : rN+1) \in \mathbb{R}^{rN\times rN}$, $\mathbf{f} = \widetilde{K}(2 : rN+1, 1) \in \mathbb{R}^{rN}$, $\mathbf{m} = \widetilde{M}(2 : rN+1, 1) \in \mathbb{R}^{rN}$, and $\mathbf{u}(t) = \{u^\sigma(\xi_i,t)\}_{i=1}^{rN} \in \mathbb{R}^{rN}$. Notice that both M and K are symmetric positive definite.

Concerning the time discretization, we focus on the time window $[0,t_f]$, for some final time, $t_f > 0$, and divide such interval in N_τ sub-intervals, identified by the time step $\tau = t_f/N_\tau$, such that $t^{n+1} = t^n + \tau$, for $n = 0,\dots,N_\tau - 1$. Then, we resort to the Newmark method [10], and in particular to its a-form implementation. This is a well-known one-step algorithm for a second-order ordinary differential system in time describing general damped/undamped structural dynamics applications [5]. In this method, system (27) is reformulated in terms of three unknowns, $\mathbf{a} = \mathbf{u}_{tt}$, $\mathbf{v} = \mathbf{u}_t$, and $\mathbf{u}$, so that it becomes

$$\begin{cases} M\mathbf{a}(t) + K\mathbf{u}(t) &= \mathbf{F}(t) \quad t \in (0,t_f] \\ \mathbf{u}(0) &= \mathbf{0} \\ \mathbf{v}(0) &= \mathbf{0}. \end{cases} \tag{28}$$

Then, equation $(28)_1$ is evaluated at the time level t^{n+1} as

$$M\mathbf{a}^{n+1} + K\mathbf{u}^{n+1} = \mathbf{F}^{n+1},$$

[1] We adopt a standard Matlab syntax to extract array components.

where the superscripts indicate the corresponding time level, supplemented with the following Taylor-like expansions to link the unknowns at t^n and at t^{n+1}:

$$\begin{cases} \mathbf{u}^{n+1} &= \underbrace{\mathbf{u}^n + \tau\mathbf{v}^n + \tau^2\big((1/2-\beta)\mathbf{a}^n}_{\mathbf{u}_p^n} + \beta\mathbf{a}^{n+1}\big) &= \mathbf{u}_p^n + \tau^2\beta\,\mathbf{a}^{n+1}, \\ \mathbf{v}^{n+1} &= \underbrace{\mathbf{v}^n + \tau\big((1-\alpha)\mathbf{a}^n}_{\mathbf{v}_p^n} + \alpha\mathbf{a}^{n+1}\big) &= \mathbf{v}_p^n + \tau\alpha\,\mathbf{a}^{n+1}. \end{cases}$$

The variables $\mathbf{u}_p^n, \mathbf{v}_p^n$ denote *predicted* values for the displacement and the velocity, respectively, and can be computed explicitly, since they depend just on the state at time level n. The Newmark one-step procedure to advance in time consists of: Given $[\mathbf{u}^n, \mathbf{v}^n, \mathbf{a}^n]$, we compute $[\mathbf{u}^{n+1}, \mathbf{v}^{n+1}, \mathbf{a}^{n+1}]$ by the following steps

$$\begin{cases} \mathbf{u}_p^n &= \mathbf{u}^n + \tau\mathbf{v}^n + \tau^2(1/2-\beta)\mathbf{a}^n \\ \mathbf{v}_p^n &= \mathbf{v}^n + \tau(1-\alpha)\mathbf{a}^n \\ (M + \tau^2\beta K)\,\mathbf{a}^{n+1} &= \mathbf{F}^{n+1} - K\mathbf{u}_p^n \\ \mathbf{u}^{n+1} &= \mathbf{u}_p^n + \tau^2\beta\,\mathbf{a}^{n+1} \\ \mathbf{v}^{n+1} &= \mathbf{v}_p^n + \tau\alpha\,\mathbf{a}^{n+1}, \end{cases}$$

where the first two and the last two assignments are straightforward vector updates. The third line involves solving an algebraic linear system for the unknown $\mathbf{a}^{n+1}$, with a symmetric positive definite matrix, being a linear combination of the stiffness and mass matrix.

After dealing with the approximation to the wave equation, we have to address the recovery of the model parameters, b, γ, by a suitable identification procedure. We summarize the overall algorithm, comprising both the approximation of the wave equation and the estimate of b and γ, in Alogorithm 1.

Some remarks are in order. The function in line 2. (and its corresponding second-order derivative in time in line 3.) replaces the impulse in (10). This is a user-defined Gaussian function, centered at $t = t_0$, with variance λ, and with unit integral over $\mathbb{R}$.
The vector function $\mathbf{F}$ in line 4. coincides with definition (27).
In lines 5.-7., according to a standard finite element approach, we introduce the local degrees of freedom (the $r+1$ uniform nodes associated with the space $\mathbb{P}^r$), on the reference unit interval, and form the corresponding global stiffness and mass matrices, by typical local-to-global assembly procedures [13]. The relation $\tau = 0.1\sigma$ reduces the dispersion error in the Newmark method.
The time marching process is carried out in lines 11.-16., via the Newmark method, after the initialization in lines 8.-9.

Algorithm 1

1. Input : $b_0, t_0, \lambda, \gamma, b, r, N, t_f, \beta, \alpha$;
2. Define : $h(t) = \frac{1}{\sqrt{2\pi}\lambda} \exp\big(\frac{-(t-t_0)^2}{2\,\lambda^2}\big)$;
3. Define : $h_{tt}(t) = \frac{(t-t_0)^2-\lambda^2}{\lambda^4}\, h(t)$;
4. Define : $\mathbf{F}(t) = -\big(h(t)\,\mathbf{f} + h_{tt}(t)\,\mathbf{m}\big)$;
5. Define : $\{\hat{x}_k\}_{k=0}^r : \hat{x}_k = k/r$;
6. Set : $\sigma = b/N;\ \tau = 0.1\sigma;\ N_\tau = t_f/\tau$;
7. Assemble : M, K as in (27);
8. Set : $n = 0;\ t^0 = 0;\ \mathbf{u}^0 = \mathbf{v}^0 = \mathbf{0};\ w^0 = 0$;
9. Solve for $\mathbf{a}^0 : M\mathbf{a}^0 = \mathbf{F}(0)$;
10. for $n = 0 : N_\tau - 1$

    % `Newmark step`

    11. $t^{n+1} = t^n + \tau$;
    12. Set : $\mathbf{u}_p^n = \mathbf{u}^n + \tau\mathbf{v}^n + \tau^2(1/2-\beta)\mathbf{a}^n$;
    13. Set : $\mathbf{v}_p^n = \mathbf{v}^n + \tau(1-\alpha)\mathbf{a}^n$;
    14. Solve for $\mathbf{a}^{n+1} : (M + \tau^2\beta K)\,\mathbf{a}^{n+1} = \mathbf{F}^{n+1} - K\,\mathbf{u}_p^n$;
    15. Set : $\mathbf{u}^{n+1} = \mathbf{u}_p^n + \tau^2\beta\,\mathbf{a}^{n+1}$;
    16. Set : $\mathbf{v}^{n+1} = \mathbf{v}_p^n + \tau\alpha\,\mathbf{a}^{n+1}$;

    % `Approximation to` $u_x(0, t^{n+1})$

    17. Compute : w^{n+1} by (29);
18. end

% `Estimate of` b, γ

19. Compute : $g(T^n)$ by (30), for $T^n \in [b_0/2 + t_0, 3b - \tau]$;
20. Compute : b by (31);
21. Compute : $\Delta = -\min_n g(T^n)$;
22. Compute : γ by (17);

To compute $g(T)$ in (13), we resort to a numerical integration formula, after replacing $u_x(0,t)$ with a suitable approximation. Concerning this last issue, the idea is first to interpolate the values $\{\tilde{\mathbf{u}}_k^{n+1}\}_{k=0}^r$, at the generic time level $n+1$, at the $r+1$ uniform nodes $\{\xi_k\}_{k=0}^r$ on the leftmost interval $[0, x_1]$, by a polynomial in $\mathbb{P}^r$. However, for numerical conditioning issues, this approximation is carried out on the reference element: Given $\{(\hat{x}_k, \tilde{\mathbf{u}}_k^{n+1})\}_{k=0}^r$, find the coefficients $\{c_k\}_{k=0}^r$ such that

$$p^r(\hat{x}_j) = \sum_{k=0}^{r} c_k\, \hat{x}_k^{r-k} = \tilde{\mathbf{u}}_j, \quad j = 0, \ldots, r.$$

The coefficients, $\{d_k\}_{k=0}^r$, of the polynomial $q^r(x) = \sum_{k=0}^{r} d_k\, x^{r-k}$ on the physical interval $[0, x_1]$ are computed by the transformation $\{d_k\}_{k=0}^r = \{c_k\sigma^{k-r}\}_{k=0}^r$. Finally, the approximation, w^{n+1}, to $u_x(0, t^{n+1})$ is computed in line 17. as

$$w^{n+1} = q_x^r(0) = d_{r-1}, \tag{29}$$

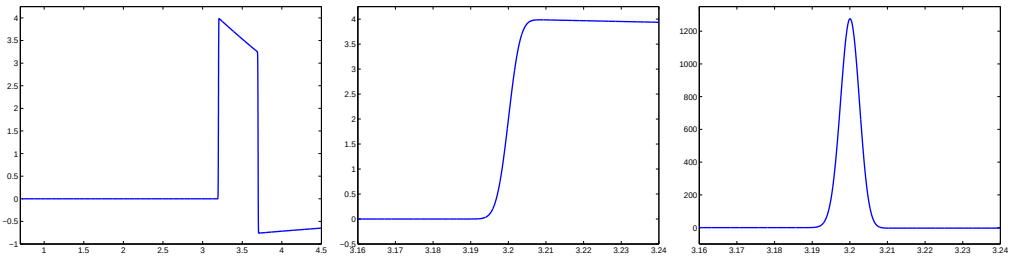

Figure 4: Test 1: Plot of $g(T^n)$ (left), of a detail (center), and of $\frac{dg}{dT}(T^n)$ (right), for $T^n \in [3.16, 3.24]$.

with

$$q_x^r(x) = \sum_{k=0}^{r-1} (r-k) d_k \, x^{r-k-1}.$$

As for the numerical integration involved in (13), we consider the interval $[b_0/2 + t_0, 3b - \tau]$ for T, and sample this interval with the same step used for the Newmark method, i.e., τ and denote by T^n the variable right endpoint in the integral in (13). Additionally, we resort to a composite quadrature rule based on the uniform nodes $\{t^n\}_{n \geq 0}$. Thus, we divide the interval $[0, T^n]$ in $N_n = T^n/\tau$ sub-intervals, and employ the composite trapezoidal quadrature rule, taking into account that $w^0 = 0$, due to the initial condition in (1). This yields the computation in line 19.

$$g(T^n) \simeq \tau \sum_{k=1}^{N_n - 1} w^k \varphi_{T^n}(t^k) + 0.5\tau \, w^{N_n} \varphi_{T^n}(t^{N_n}). \tag{30}$$

We are now ready to compute the pair (b, γ) in lines 20.-22., inspired by (18)-(19). In particular, b is derived by computing first $T_M = \arg\max_n \frac{dg}{dT}(T^n)$ in a neighborhood of the positive steep gradient of g, and then the quantity

$$b = 0.5(T_M - t_0). \tag{31}$$

As for γ, we exploit (17) after properly approximating Δ in (16), as the minimum of $g(T^n)$ over the interval $[b_0/2 + t_0, 3b - \tau]$, up to the sign.

A numerical assessment. We now carry out two numerical experiments, corresponding to the data in Fig. 2. Concerning the configuration on the left, we pick the input parameters to Algorithm 1: $b_0 = 1$, $t_0 = 0.2$, $\lambda = 0.0025$, $\gamma = 0.2$, $b = 1.5$, $r = 2$, $N = 6000$, $t_f = 3b + 2t_0 = 4.7$, $\beta = 1/4$, $\alpha = 1/2$. For estimating b, we consider the plot of g in Fig. 4 (left), and zoom in on around the first discontinuity, in Fig. 4 (center). With high confidence, we can state that $3.19 < 2b + t_0 < 3.21$. The derivative of $g(T)$, represented in this interval in Fig. 4 (right), predicts $T_M = 3.200075$, from which we can recover the value $b = 1.5000375$, which is a very accurate approximation to the exact value.

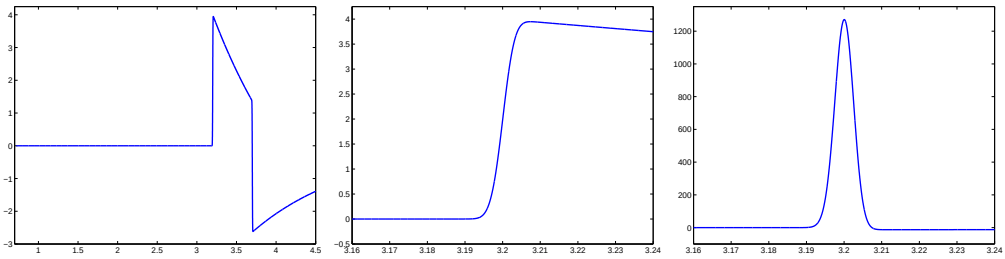

Figure 5: Test 2: Plot of $g(T^n)$ (left), of a detail (center), and of $\frac{dg}{dT}(T^n)$ (right), for $T^n \in [3.16, 3.24]$.

The computed value in line 21., based on Fig. 4 (left), is $\Delta = 0.759734$, which yields the estimated value $\gamma = 0.199567$, very close to the exact value, differing only by circa 0.2% with respect to a relative error.

Figure 5 collects the results associated with the configuration on the right in Fig. 2. The same parameters as in the previous case are chosen, except for γ, set to 0.8. The estimated values of the parameters are $T_M = 3.200050$, $b = 1.5000250$, and $\Delta = -2.618865$, $\gamma = 0.793084$, with a relative error on this latter of about 0.8%.

5 Conclusions

The exact solvability of the linear wave equation in a one-dimensional setting turns out to be a non-trivial issue when the spatial interval is bounded and mixed-boundary conditions complete the problem. In particular, the Robin data makes the problem more challenging with a view to the computation of the solution in closed form. Indeed, the constructive procedure used in the proof to Proposition 2.1, although based on the standard method of characteristics, demands a particular care due to the boundedness of the spatial domain. In principle, we can extend the solution to larger times, though the technicalities become more involved.

The reconstruction formulas (18)-(19) provide a practical way to compute the unknown parameters. This is corroborated by the numerical investigation in Section 4, which shows that the accuracy of the recovered parameters is high, thus assessing the reliability of Algorithm 1. The regularization of the Dirichlet data (i.e., the replacement of the impulsive signal with a Gaussian function) required by the numerical procedure can be conceived as a possible physical effect due to measurement errors. Nevertheless, this smoothing does not spoil the physics of the problem, thanks to both a stable recovery procedure (as shown in Section 3.1) and a robust numerical scheme (the Newmark finite element method).

References

[1] Handbook of Acoustics, M. J. Crocker, Ed., John Wiley & Sons, Inc., 1998.

[2] V. Bacchelli, M. Di Cristo, E. Sinchich and S.Vessella, A parabolic inverse problem with mixed boundary data. Stability estimates for the unknown boundary and impedance. *Trans. Amer. Math. Soc.* **366**(8) (2014), 3965–3995.

[3] A. Doubova and E. Fernandez-Cara, Some geometric inverse problems for the linear wave equation, *Inv. Probl. and Imaging* **9** (2015), 371–393.

[4] L. C. Evans, *Partial Differential Equations*, Graduate Studies in Mathematics, 19, American Mathematical Society, Providence, Rhode Island, 2010.

[5] T. J. H. Hughes, *The Finite Element Method. Linear Static and Dynamic Finite Element Analysis*, Dover Publications, Inc., Minneola, New York, 2000.

[6] M. Ikawa, *Hyperbolic partial differential equations and wave phenomena*, in Translations of Mathematical Monographs **189** (Iwanami Series in Modern Mathematics), American Mathematical Society, 2000.

[7] C. Isakov, On uniqueness of obstacles and boundary conditions from restricted dynamical and scattering data, *Inv. Probl. and Imaging* **2** (2008), 151–165.

[8] D. Lesnic, S. O. Hussein and B. T. Johansson, Inverse space-dependent force problems for the wave equation, *J. Comput. Appl. Math.* **306** (2016), 10–39.

[9] S.-W. Na and L. F. Kallivokas, Direct time-domain soil profile reconstruction for one-dimensional semi-infinite domains, *Soil Dyn. Earthq. Eng.* **29** (2009), 1016–1026.

[10] N. M. Newmark, A method of computation for structural dynamics, *J. Eng. Mech. Div.*, ASCE, (1959), 67–94.

[11] A. N. Tikhonov and A. A. Samarskii, *Equations of Mathematical Physics*, Dover Publications, Inc., New York, 1990.

[12] G. Q. Xie, A new iterative method for solving the coefficient inverse problem of the wave equation, *Comm. Pure Appl. Math.* **39** (1986), 307–322.

[13] O. C. Zienkiewicz, R. L. Taylor and J. Z. Zhu, *The Finite Element Method: Its Basis and Fundamentals*, Elsevier/Butterworth-Heinemann, Amsterdam, Seventh Edition, 2013.

MOX Technical Reports, last issues

Dipartimento di Matematica
Politecnico di Milano, Via Bonardi 9 - 20133 Milano (Italy)

29/2017 Antonietti, P.F.; Mascotto, L.; Verani, M.
A multigrid algorithm for the p--version of the Virtual Element Method

27/2017 Bonaventura, L.; Ferretti, R.; Rocchi L.;
A fully semi-Lagrangian discretization for the 2D Navier--Stokes equations in the vorticity--streamfunction formulation

28/2017 Pini, A.; Spreafico, L.; Vantini, S.; Vietti, A.
Multi-aspect local inference for functional data: analysis of ultrasound tongue profiles

26/2017 Masci, C.; Johnes, G.; Agasisti, T.
Student and School Performance in the OECD: a Machine Learning Approach.

25/2017 Paulon, G.; De Iorio, M.; Guglielmi, A.; Ieva, F.
Joint modelling of recurrent events and survival: a Bayesian nonparametric approach

24/2017 Domanin, M.; Bissacco, D.; Le Van, D.; Vergara, C.
Computational fluid-dynamic comparison between patch-based and direct suture closure techniques after carotid endarterectomy

23/2017 Quarteroni, A.; Vergara, C.
Computational models for hemodynamics

21/2017 Talska, R.; Menafoglio, A.; Machalova, J.; Hron, K.; Fiserova, E.
Compositional regression with functional response

22/2017 Bartezzaghi, A.; Dede', L.; Quarteroni, A.
Biomembrane modeling with Isogeometric Analysis

20/2017 Albrecht G.; Caliò F.; Miglio E.
Fair surface reconstruction through rational triangular cubic Bézier patches